

Acta Cryst. (1969). B25, 2423

An X-ray Study of α -Oxalic Acid Dihydrate, $(\text{COOH})_2 \cdot 2\text{H}_2\text{O}$, and of its Deuterium Analogue, $(\text{COOD})_2 \cdot 2\text{D}_2\text{O}$: Isotope Effect in Hydrogen Bonding and Anisotropic Extinction Effects

BY ROBERT G. DELAPLANE AND JAMES A. IBERS

Department of Chemistry and Materials Research Center, Northwestern University, Evanston, Illinois 60201, U.S.A.

(Received 10 January 1969)

A three-dimensional X-ray diffraction study of the α -modification of both $(\text{COOH})_2 \cdot 2\text{H}_2\text{O}$ and $(\text{COOD})_2 \cdot 2\text{D}_2\text{O}$ has been made. For each substance, intensity data were collected with Cu $K\alpha$ radiation out to 110° in 2θ on a Picker automatic diffractometer. Positional and anisotropic thermal parameters for all atoms were refined on F^2 by full-matrix least-squares techniques. A correction for anisotropic extinction effects was included in the least-squares refinement. The weighted R factors on F^2 are 3.9% (547 observed reflections) for α - $(\text{COOH})_2 \cdot 2\text{H}_2\text{O}$ and 3.9% (555 observed reflections) for α - $(\text{COOD})_2 \cdot 2\text{D}_2\text{O}$. The corresponding conventional R factors on F^2 are 2.8% and 2.8% respectively; on F they are 2.0% and 2.3%. The oxalic acid molecules and water molecules are linked together by a three-dimensional network of hydrogen bonds. All three crystallographically independent O—H...O bond lengths expand significantly with deuteration while the bond lengths within the oxalate fragment remain unchanged. In α - $(\text{COOH})_2 \cdot 2\text{H}_2\text{O}$, the O—H...O distances are 2.512 (1), 2.864 (2) and 2.883 (1) Å; the corresponding O—D...O distances in α - $(\text{COOD})_2 \cdot 2\text{D}_2\text{O}$ are 2.531 (1), 2.880 (2) and 2.907 (1) Å.

Introduction

Extensive studies have been made on the structural effects of deuterium substitution in hydrogen bonded solids. New polymorphs have been formed by deuterating potassium dihydrogen phosphate (Ubbelohde & Woodward, 1942), resorcinol (Robertson, 1936; Robertson & Ubbelohde, 1938) and oxalic acid dihydrate (Chiba, 1964; Iwasaki & Saito, 1967; Iwasaki, Iwasaki & Saito, 1967). Smaller effects have been found in investigations of isomorphous protonated and deuterated analogues of several compounds. A summary of these results shows several examples where the replacement of H by D produces a marked expansion of the crystal lattice (Ubbelohde & Gallagher, 1955; Ibers, 1965). From a knowledge of the protonated structure and the measured changes in the unit-cell dimensions on deuteration, Ubbelohde and co-workers found the directions of maximum expansion nearly to coincide with the directions of short hydrogen bonds in the lattice. By assuming the isotope effect to be localized in the hydrogen bonds, they calculated the differences in the corresponding O—H...O and O—D...O distances from the expansion coefficient in the direction of the bonds. They concluded that large isotope effects were observed only in short hydrogen bonds while deuteration had little or no effect on long hydrogen bonds. These conclusions are not unambiguous since many of the solids studied contain more than one crystallographically independent hydrogen bond. A determination of the atomic positions in the deuterated crystals was not attempted, as the precision obtainable at that time was too low to allow meaningful comparisons between the hydrogen and deuterium structures.

Crystals of deuterated oxalic acid dihydrate, $(\text{COOD})_2 \cdot 2\text{D}_2\text{O}$ (hereafter called α -DOX), were found

by Robertson & Ubbelohde (1939) to be isomorphous with those of $(\text{COOH})_2 \cdot 2\text{H}_2\text{O}$ (hereafter called α -POX) (Robertson & Woodward, 1936; Ahmed & Cruickshank, 1953; Garrett, 1954) and to exhibit a large isotope effect. Recently the crystal structure of a new modification of $(\text{COOD})_2 \cdot 2\text{D}_2\text{O}$ was reported (hereafter called β -DOX) (Iwasaki & Saito, 1967; Iwasaki, Iwasaki & Saito, 1967) which is not isomorphous with that of α -DOX. In order to determine the exact nature of the isotope effect in α -DOX, a three-dimensional X-ray analysis was made of the crystal structures of both α -POX and α -DOX. A preliminary report of the present work has previously appeared (Delaplane & Ibers, 1966). The present paper is the first in a series of four papers. The next paper describes a neutron diffraction study of α -POX (Sabine, Cox & Craven, 1969); it is followed by a description of a neutron diffraction study of α -DOX and β -DOX (Coppens & Sabine, 1969) and in the final paper (Coppens, Sabine, Delaplane & Ibers, 1969) some comparisons are made between the X-ray and neutron results on oxalic acid dihydrate and their implications in terms of bonding effects are discussed.

Experimental

Crystals of α -POX were recrystallized from aqueous solution. About 0.35 g of anhydrous oxalic acid was dissolved in 2 ml of 99.85 mole% D_2O with heating, and the water was evaporated in vacuo. After repeating the procedure three times, a final recrystallization yielded crystals of α -DOX. Crystals of both substances were colorless monoclinic needles with the needle axis coincident with the b axis. Recrystallization of oxalic acid dihydrate from D_2O has also been reported to produce rhomboidal crystals of β -DOX (Iwasaki & Saito, 1967; Iwasaki *et al.*, 1967; Coppens & Sabine, 1969). The pres-

ent work deals only with the α -form. The crystal data of both α -POX and α -DOX are listed in Table 1. The unit-cell dimensions were obtained at 26°C with the least-squares procedure described below [$\lambda(\text{Cu } K\alpha_1) = 1.5405 \text{ \AA}$].

Table 1. *Crystal data**

Space group	α -(COOH) ₂ ·2H ₂ O <i>P</i> 2 ₁ / <i>n</i>	α -(COOD) ₂ ·2D ₂ O <i>P</i> 2 ₁ / <i>n</i>
<i>a</i>	6.119 (1) Å	6.150 (1) Å
<i>b</i>	3.607 (1)	3.612 (1)
<i>c</i>	12.057 (1)	12.102 (1)
β	106° 19 (1)′	106° 38 (1)′
<i>Z</i>	2	2
<i>V</i>	255.4 Å ³	257.6 Å ³

* Numbers in parentheses here and in succeeding Tables are the estimated standard deviations in the least significant digits.

Collection and reduction of data

α -DOX

A needle-shaped crystal with an average diameter of about 0.22 mm and a length of 0.45 mm was mounted in a thin glass capillary to prevent dehydration and deuterium-hydrogen exchange with the air. For subsequent absorption and extinction corrections, the crystal faces were indexed, and the crystal was measured. These measurements are given in Table 2. For data collection, the crystal was mounted about the *b* axis on a Picker four-circle automatic X-ray diffractometer. The arcs on the goniometer were then changed several degrees so that the crystal would not be oriented about the symmetry axis, thus minimizing the possibility of multiple reflections (Zachariasen, 1965). The mosaicity of the crystal was judged to be satisfactory upon checking ω scans of several strong reflections by the narrow-source, open-counter technique (Furnas, 1957). The average half-width was about 0.09°. A group of high-angle reflections was carefully centered using a narrow receiving slit and a narrow X-ray source as provided by a take-off angle of 0.5° for the X-ray tube. The lattice constants and the orientation angles were obtained from a least-squares refinement using the observed angle settings for each reflection as input data (Corfield, Doedens & Ibers, 1967).

Table 2. *Crystal dimensions*

α -DOX		α -POX	
<i>hkl</i> *	<i>D</i> †	<i>hkl</i> *	<i>D</i> †
001	0.113	001	0.133
00 $\bar{1}$	0.113	00 $\bar{1}$	0.133
101	0.138	101	0.124
$\bar{1}0\bar{1}$	0.138	$\bar{1}0\bar{1}$	0.124
10 $\bar{1}$	0.103	10 $\bar{1}$	0.087
$\bar{1}01$	0.103	$\bar{1}01$	0.087
1 $\bar{2}1$	0.231	010	0.206
$\bar{1}2\bar{1}$	0.231	0 $\bar{1}0$	0.206
Crystal volume‡	0.02297 mm ³		0.01856 mm ³

* Indices of each bounding plane.

† Perpendicular distance in millimeters of each plane from an origin at the center of the crystal.

‡ These values were calculated with the data processing and absorption correction program *DATAP* written by Coppens *et al.* (1965).

The intensity data were collected at a take-off angle of 1.2°. At this angle the intensity of a typical strong reflection was approximately 75% of the maximum value as a function of take-off angle. The scintillation counter was placed 21 cm from the crystal with a receiving aperture size of 5.0 mm wide and 4.0 mm high to minimize extraneous background radiation. The diffracted Cu *K* α beam was filtered through a 1.0 mil nickel foil. Integrated intensities were collected using the θ -2 θ continuous scan technique. A symmetrical scan range of 2° in 2 θ was used, and the scan rate was 2° min⁻¹. Stationary-counter background counts of 4 seconds were taken at each end of the scan range. Copper foil attenuators were automatically inserted when the intensity of the diffracted beam exceeded about 7000 counts sec⁻¹ during the scan. The attenuator factors were about 2.3. The pulse height analyzer was set to accept about a 95% window centered on the Cu *K* α peak.

The intensities of all four equivalent members (*hkl*, $\bar{h}\bar{k}\bar{l}$, *h* \bar{k} \bar{l} , $\bar{h}k\bar{l}$) of the form {*hkl*} were collected. Since in our procedure for data collection (Corfield, Doedens & Ibers, 1967) the reflections are ordered in an attempt to minimize slewing times of the drive motors, the equivalent members of a given form typically are collected at widely varying times during the period of data collection. The intensities of four standard reflections were checked periodically during the run to monitor diffractometer and crystal stability. No significant changes were observed in these standards. A total of 941 intensities were measured out to a 2 θ value of 110° for Cu *K* α (hereafter called Data Set 1).

The procedure used in processing the data is similar to that previously described by Corfield, Doedens & Ibers (1967). The raw intensities were corrected for background, which was assumed to vary linearly throughout the scan range. Standard deviations were assigned to the corrected intensities through the expression

$$\sigma(I) = [CT + (t_p/2t_b)^2 (B_1 + B_2) + (pI)^2]^{1/2}$$

where *CT* is the total integrated peak count measured in time *t_p*, *B*₁ and *B*₂ are the background counts, each measured in time *t_b*, and *I* = *CT* - (*t_p*/2*t_b*) (*B*₁ + *B*₂). The inclusion of the term (*pI*)² prevents intense reflections from being overweighted (Busing & Levy, 1957). An initial value of 0.03 was chosen for *p*, based on past experience with similar data sets. The values of *I* and $\sigma(I)$ were corrected for Lorentz-polarization and absorption effects. The absorption correction was effected by numerical methods. For a calculated absorption coefficient of 15.8 cm⁻¹, the transmission factor *A** varied from 0.77 to 0.68. The values of *F*² for each equivalent set of reflections were averaged to yield 323 independent reflections, of which 15 were less than their standard deviations. Standard deviations of *F*², $\sigma(F^2)$, were estimated from both the average of the individual standard deviations and from the range of *F*² values of the equivalent members of the form. The larger of

the two estimated values was chosen and was divided by $n^{1/2}$, where n is the number of equivalent members which were observed for that reflection (Robinson & Ibers, 1967). If $\sigma(F^2)$ is assumed to be a measure of $|F_o^2 - F_c^2|$, a predicted weighted R factor (R_2) may be computed from the F^2 and $\sigma(F^2)$ values. The predicted R_2 factor on F^2 of 3.8% indicates good agreement among equivalent members of the form $\{hkl\}$.

Because many of the most intense reflections in Data Set 1 were subsequently found to be severely attenuated by extinction effects, a supplementary data set was collected on a smaller crystal, a needle with an average diameter of 0.040 mm and a length of 0.16 mm. Following the above procedure, a symmetrical scan range of 1.8° was used with a scan rate of 1° min^{-1} and 10 sec background counts. During the period of data collection, which lasted 26 hours, the monitored intensities of the same four standard reflections used for Data Set 1, uniformly decreased by 15%. This was attributed to partial decomposition of the crystal. A total of 453 intensities consisting of all four members of the form $\{hkl\}$ were measured out to a 2θ value of 80° for Cu $K\alpha_1$ (hereafter called Data Set 2). Beyond this maximum 2θ value, there were very few reflections with $F^2 > \sigma(F^2)$.

The raw intensities in Data Set 2 were corrected for the effects of background, Lorentz-polarization, and absorption. The average decrease in the intensities of the four standard reflections as a function of time was used as the correction factor for the intensity loss during data collection. The individual F^2 values were averaged using the above procedure with a value of 0.01 for p . A total of 152 independent reflections was obtained of which 79 were less than their standard deviations.

α -POX

The procedure for collecting and processing the data parallels the one previously outlined for α -DOX, and only differences will be emphasized. A needle-shaped crystal with an average diameter of about 0.23 mm and a length of 0.41 mm was chosen for data collection. The measured dimensions of the crystal are given in Table 2. The average half-width of ω scans of several strong reflections was about 0.08° . Integrated intensities were collected using the θ - 2θ continuous scan technique with a symmetrical scan range of 2° in 2θ and a scan rate of 2° min^{-1} . Stationary-counter background counts of 4 sec were taken at each end of the scan range. A total of 932 intensities consisting of all four members of the form $\{hkl\}$ were measured out to a 2θ value of 110° for Cu $K\alpha_1$ (hereafter called Data Set 1).

Four standard reflections were used to monitor the stability of both the crystal and the diffractometer. During the 45 hour period of data collection, the intensity of the standard 110 reflection was observed to increase by 15% with no significant drift in the intensities of the other three standards. After continuously irradiating the crystal with the X-ray beam for an addi-

tional 20 hours, the intensity of reflection 110 continued to increase and then leveled off at about 1.25 times its original value. Only very small increases were noted in the other three standards. No further observable intensity changes in any of the standard reflections were noted after dipping the crystal several times in liquid nitrogen. The reflection 110 is the most intense in the data set, while the other standards are only moderately strong. These intensity changes were interpreted as being due to extinction effects. In general, extinction effects are most prominent in the most intense reflections and depend upon the mosaic spread of the crystal. The continuous radiation damage to the crystal increased the mosaic spread as a function of time, thus increasing the observed intensities of the most intense reflections.

The raw intensities were corrected for background, Lorentz-polarization, and absorption effects and were then averaged. For a calculated absorption coefficient of 15.8 cm^{-1} , the transmission factor A^* ranged from 0.76 to 0.68. No attempt was made to correct for the intensity changes which occurred during data collection. For assigning the standard deviations, an initial value of 0.05 was used as the p factor. Of 321 independent F^2 values, 15 were less than their standard deviations. The predicted R_2 factor on F^2 was 5.9%.

A supplementary data set was collected on a smaller needle-shaped crystal with an average diameter of 0.09 mm with a length of 0.21 mm. Following the above procedure, a symmetrical scan range of 1.8° was used with a scan rate of 2° min^{-1} and 4 sec stationary-counter background counts. No change was observed in the intensities of the monitored standard reflections during the period of data collection. A total of 440 intensities consisting of all four equivalent reflections of the form $\{hkl\}$ were measured out to a 2θ value of 80° for Cu $K\alpha_1$ (hereafter called Data Set 2).

The raw intensities in Data Set 2 were corrected for background, Lorentz-polarization, and absorption effects and were averaged. A value of 0.015 was used for the p factor in assigning $\sigma(F^2)$ values. Of 150 independent F^2 values, 19 were less than their standard deviations.

It is important to reiterate that in the data sets obtained here the intensities of members of a given form were collected at widely varying times during a given experiment and that the standard deviation of the average intensity was assigned on the basis of the agreement among the intensities of the individual members of the form. Thus resultant weighting scheme effectively allows for the effects of possible crystal decomposition during the experiment.

Initial refinements of the structures

α -DOX

Using only the F^2 values of Data Set 1, a least-squares refinement on F^2 was carried out. In all calculations of F_o^2 , the atomic scattering factors tabulated by Ibers (1962) were used for C and O and those of Stewart, Davidson & Simpson (1965) were used for H (and D).

The initial parameters were those reported by Ahmed & Cruickshank (1953) for C and O and those of Garrett (1954) for H. Positional parameters and anisotropic thermal parameters for each atom and an overall scale factor were refined. The function $\sum w(F_o^2 - F_c^2)^2$ was minimized with the weights w taken as $1/\sigma^2(F^2)$. After three cycles of least-squares refinement, carried out with a local modification of the Busing-Levy *ORFLS* program, the usual agreement indices $R_1 = \sum(F_o^2 - F_c^2)/\sum F_o^2$ and $R_2 = [(\sum w(F_o^2 - F_c^2)^2)/\sum w F_o^4]^{1/2}$ were 17.2 and 12.9% respectively. The predicted R_2 value of 3.8%, indicative of good agreement among equivalent members of the form $\{hkl\}$, suggested that the structure was still underrefined. For several intense reflections at low values of $\lambda^{-1} \sin \theta$, F_o^2 was consistently less than F_c^2 suggesting that these reflections may be severely attenuated by extinction.

An extinction correction of the form $(F_o^{\text{corr}} = y)F_o$ where $y = \{C\beta(2\theta)I_{\text{obs}} + [1 + C^2\beta^2(2\theta)I_{\text{obs}}^2]^{1/2}\}^{-1}$ was applied (Zachariasen, 1968). I_{obs} is the observed intensity, C is the variable extinction coefficient, and $\beta(2\theta)$ is the function $2(1 + \cos^2 2\theta)/(1 + \cos^2 2\theta)^2$. The quantity $\sum w(F_o^2 - F_c^2/y^2)^2$ was minimized. This procedure is similar to the first-order secondary extinction correction given by Zachariasen (1963), only here the term $dA^*/d(\mu R)$ is assumed to have a constant value of 1.0. Three cycles of least-squares refinement yielded a value for C of $2.78(13) \times 10^{-4}$ (in absolute units) and values for R_1 and R_2 of 5.6 and 6.3% respectively.

The largest increase for any reflection due to the extinction correction was about 80% of the original F_o^2 value for the reflection 110. In general, most of the large corrected F_o^2 values for reflections of the form $\{hkl\}$

($k \neq 0$) appeared to be over-corrected while those of the form $\{h0l\}$ appeared to be under-corrected. A similar trend was subsequently found to exist in the F_o^2 and F_c^2 values for α -POX using the same method of correction. This anisotropic effect could possibly be explained by anisotropic extinction or by crystal-shape effects. The above approximate form of the extinction correction assumes the crystal to be spherical in shape and assumes that the misalignment of the crystal domains obeys an isotropic Gaussian distribution law.

Hamilton (1957) has found that secondary extinction coefficients can be very sensitive to the shape of the crystal and to the direction of the incident X-ray beam relative to the crystal faces. The program *GONO9* of Hamilton can be used to apply an isotropic extinction correction by numerical integration procedures for crystals of any well-defined shape. The raw intensity data in Data Set 1 were reprocessed using a value for p of 0.01 as judged by the good agreement among the equivalent members of the forms in the previously averaged data set. The individual F^2 values were corrected for absorption and extinction effects with the program *GONO 9*, which had been modified to include the polarization term in the extinction correction for the X-ray case (Zachariasen, 1963). A value for the extinction parameter was estimated, and after averaging the symmetry-related values of F^2 , a least-squares refinement of all the structural parameters was then made. The process was repeated until a value for the extinction parameter was found which would produce the lowest value for R_2 . For an extinction coefficient of 0.0130 cm^{-1} , the values for R_1 and R_2 were 5.5 and 5.0% respectively. The agreement was slightly better than in the

Table 3. Extinction parameters for α -DOX

	Isotropic	Anisotropic crystal Type I	Anisotropic crystal Type II
Isotropic g or G_{11}^*	0.400 (15)	0.010 (10)	4.08 (40)
G_{22}		0.242 (16)	15.96 (148)
G_{33}		0.041 (18)	4.32 (40)
G_{12}		0.002 (7)	-0.04 (74)
G_{13}		0.055 (14)	-1.91 (32)
G_{23}		0.007 (11)	-0.51 (67)

* The values of g and G_{ij} have been multiplied by 10^4 .

Table 4. Final positional and thermal parameters for α -DOX*

	10^4x	10^4y	10^4z	$10^4\beta_{11}\dagger$	$10^4\beta_{22}$	$10^4\beta_{33}$	$10^4\beta_{12}$	$10^4\beta_{13}$	$10^4\beta_{23}$
C(1)	-452 (2)	545 (3)	507 (1)	183 (3)	588 (11)	44 (1)	-6 (5)	23 (1)	-3 (2)
O(1)	855 (1)	-610 (3)	1477 (1)	257 (3)	1041 (11)	38 (1)	149 (4)	28 (1)	11 (2)
O(2)	-2186 (1)	2297 (2)	360 (1)	234 (3)	994 (10)	50 (1)	162 (4)	40 (1)	13 (2)
O(3)	-4496 (2)	-3853 (4)	1808 (1)	238 (4)	1025 (16)	49 (1)	102 (5)	37 (1)	21 (3)
D(1)	4632 (20)	4894 (44)	2943 (13)	277 (54)	1434 (184)	63 (14)	33 (77)	-84 (21)	-82 (43)
D(2)	554 (23)	1564 (45)	3787 (16)	289 (60)	1681 (233)	93 (16)	-196 (84)	51 (26)	-6 (47)
D(3)	-3878 (35)	4510 (51)	1604 (19)	801 (108)	1043 (243)	151 (24)	326 (118)	-95 (39)	206 (6)

* The anisotropic crystal Type II extinction correction was applied in this refinement.

† The form of the anisotropic thermal ellipsoid is

$$\exp [-(\beta_{11}h^2 + \beta_{22}k^2 + \beta_{33}l^2 + 2\beta_{12}hk + 2\beta_{13}hl + 2\beta_{23}kl)].$$

the crystal used for the supplementary data collection was small enough to minimize extinction effects, the counting statistics for even the most intense reflections were very poor owing to the small reflecting power of the crystal.

α -POX

With the use of the α -DOX parameters as initial values, a least-squares refinement on F^2 was made for α -POX using only Data Set 1. The refinement procedure parallels the one previously outlined for α -DOX, and only differences will be emphasized. Positional parameters and anisotropic thermal parameters for each atom and an overall scale factor were refined for three cycles. The values for R_1 and R_2 were 19.5 and 14.8% respectively. A comparison with the predicted R_2 value of 5.9% suggested that the structure was still under-refined. The largest F_o^2 values at low angles were consistently less than the corresponding values for F_c^2 . The F_o^2 values were corrected with the Zachariasen extinction correction previously described. Three cycles of least-squares refinement, which included the extinction coefficient as a variable, yielded a value for C of $3.65(20) \times 10^{-4}$ (in absolute units) and values for R_1 and R_2 of 9.8% and 8.1% respectively.

A comparison of the corresponding F_o^2 and corrected F_c^2 values indicated that the same anisotropic extinction effects were present here as for the larger α -DOX crystal. For these reasons the raw intensity data were reprocessed ($p=0.015$), and the resulting F^2 values were corrected for absorption and extinction with the program *GONO 9*. An extinction parameter of 0.0155 cm^{-1} was found to give the lowest value for R_2 .

The F^2 values corresponding to the four equivalent members of the form $\{hkl\}$ were averaged, and the structural parameters were refined by least-squares techniques. Three cycles of refinement led to values for R_1 and R_2 of 9.4 and 5.5% respectively.

The value for R_2 was still less than a predicted value of 2.7% derived from the new weighting scheme, and agreement between the most intense F_o^2 and F_c^2 values was still poor, perhaps because of the large magnitude of the correction. All F^2 values having $F^2 > 3\sigma(F^2)$ in Data Set 2 were used to replace the corresponding values in Data Set 1. The merged data set consisted of 321 independent reflections of which 114 were from Data Set 2 and 207 from Data Set 1. Several intense re-

flections in Data Set 2 were subsequently found to be slightly affected by extinction. Both data sets were separately corrected for extinction with the program *GONO-9*. Extinction coefficients of 0.0200 and 0.0093 cm^{-1} were chosen for Data Set 1 and Data Set 2 respectively, which gave the lowest value for R_2 for the merged data set. Three cycles of anisotropic least-squares refinement varying a separate overall scale factor for each data set gave the values for R_1 and R_2 of 4.2 and 4.4% respectively. The present experience of collecting supplementary data sets on small crystals is not wholly satisfactory. It is difficult, if not impossible, to find crystals of α -POX and α -DOX which are small enough for extinction to be negligible and yet reflecting power to be substantial.

Corrections for anisotropic extinction

Recently, Zachariasen's theory of extinction was extended to include the anisotropic case (Coppens & Hamilton, 1969) and an anisotropic extinction correction has been incorporated into the least-squares program. This technique has been applied to the present data sets.

α -DOX

The raw intensities of Data Set 1 were reprocessed as previously described. In assigning standard deviations, a value for p of 0.005 was used. This effectively increases the weights of the strongest reflections. This lower value was used since presumably the extinction present in the most intense reflections can now be corrected more effectively than before. The values of I and $\sigma(I)$ were corrected for Lorentz-polarization and absorption effects (Coppens, Leiserowitz, & Rabinovich, 1965). The intensities of only the two equivalent members (hkl) and ($\bar{h}\bar{k}\bar{l}$) of the form $\{hkl\}$ were averaged since anisotropic extinction effects may not necessarily conform to the symmetry operations of the space group. Since the crystal had a morphological center of symmetry, the extinction correction was assumed to be the same for the reflections (hkl) and ($\bar{h}\bar{k}\bar{l}$). The original 941 intensities were thus reduced to 581 independent reflections. The R_2 factor on F^2 for averaging was 1.4%. The structural parameters were again refined on F^2 using a least-squares technique similar to that previously described. The form factors of Hanson, Herman Lea & Skillman (1964) for C and O and of Stewart *et al.* (1965) for H(D) were used in all calculations of

Table 6. Extinction parameters for α -POX

	Isotropic	Anisotropic crystal Type I	Anisotropic crystal Type II
Isotropic g or G_{11} *	0.510 (23)	-0.077 (14)	2.22 (19)
G_{22}		0.447 (32)	21.34 (200)
G_{33}		0.013 (26)	1.68 (18)
G_{12}		-0.006 (8)	-1.49 (74)
G_{13}		0.073 (17)	0.10 (12)
G_{23}		0.005 (17)	-1.03 (77)

* The values of g and G_{ij} have been multiplied by 10^4 .

F_c^2 . A reflection was considered to be unobserved if $I_o < 1.5\sigma(I_o)$. For such reflections, a term $\Delta(F^2) = 1.5\sigma(F_o^2) - F_c^2$ was included in the refinement whenever $F_c^2 > 2.0\sigma(F_o^2)$.

The applied extinction correction was of the form $(F_o^{\text{corr}}) = yF_o$ where here

$$y = \left[1 + \frac{2\bar{T}(p_2/p_1^2)F_c^2g}{V \sin 2\theta} \right]^{1/2}$$

\bar{T} is the mean path length through the crystal for each reflection and has been modified for absorption effects through the approximation $\bar{T} \simeq (-\log A^*)/\mu$ where A^* is the transmission factor and μ is the linear absorption coefficient. For unpolarized X-rays, $p_n = (1 + \cos^2 2\theta)/2$ and $(V = V_{\text{cell}}^2/\lambda^3) \times 10^{-4} \times 12.593$ where the quantity 12.593 is $(mc^2/e^2)^2$. The extinction parameter g may be constant for all reflections in the isotropic case or may be derived from a tensor in the anisotropic case. This tensor may take two different forms since the extinction may be dominated by either the mosaic spread (Type I crystal) or the average domain size (Type II crystal). For Type I crystals, an anisotropic Gaussian mosaic spread distribution is assumed to be described by a tensor \mathbf{G}_{ij} : $g = (N' \mathbf{G} N)^{1/2}$ where N_i are the components of a unit vector normal to the plane containing the incident and diffracted beams. The components are defined relative to axes of unit length which are parallel to the real crystal axes. For Type II crystals, the average mosaic particle is ellipsoidal in shape and is described again by a tensor \mathbf{G}_{ij} : $g = (M' \mathbf{G} M)^{-1/2}$ where M_i are the components of a unit vector in the plane of the incident and diffracted beams and perpendicular to the incident beam. The components M_i are defined relative to a set of unit axes parallel to the real crystal axes.

Atomic positional and anisotropic thermal parameters for each atom, an overall scale factor, and the isotropic extinction coefficient g were refined for four cycles yielding values of 4.1 and 4.6% for R_1 and R_2 respectively. The final value for g is included in Table 3. The isotropic value for g was then converted to the six components G_{ij} of the tensor describing a three-dimensional Gaussian for a Type I crystal. These six components and the usual structural parameters were refined for 7 cycles. The values for R_1 and R_2 dropped to 2.5 and 4.0% respectively. The values for the components G_{ij} are given in Table 3. The isotropic value for g was then converted to the six components G_{ij} of the tensor describing the ellipsoidal shape of an average mosaic

particle which characterizes the anisotropic extinction in a Type II crystal. These six components and the structural parameters were refined for 9 cycles yielding values of 2.8 and 3.9% for R_1 and R_2 , respectively. The final values for the components G_{ij} are included in Table 3. In the final cycle of all of the three above refinements, no shift in any parameter was larger than a standard deviation. No attempts were made to carry out refinements on a merged data set which would include intensities from Data Set 2.

From a comparison of the various values for R_2 , the structural parameters for the anisotropic Type II refinement were chosen as the best model which characterizes the extinction in this particular crystal. Clearly, there is very little difference in agreement between the models for Type I and Type II crystals. A proper description probably lies somewhere between these two models. The atomic positional and thermal parameters derived from the last cycle of the anisotropic Type II refinement are presented in Table 4, along with the corresponding standard deviations in these parameters as derived from the inverse matrix. These parameters correspond to values for R_1 and R_2 (based on F) of 2.3 and 2.0% respectively. The values for $100|F_o|$ (corrected for extinction) and $100|F_c|$ (in electrons) are given in Table 5.

The agreement in the atomic positional and thermal parameters among the latter three refinements is well within the combined standard deviations for each parameter. Among all of the refinements, corresponding positional parameters usually differ by no more than twice their combined standard deviations. Thermal parameters increase as much as five standard deviations in going from the uncorrected refinement to refinements where extinction corrections were made. Differences in the structural parameters among the various refinements are attributed to differences in extinction models and weighting scheme (different values for p). It is important to note that although corrections for extinction are necessary to obtain accurate thermal parameters positional parameters are rather insensitive to such corrections.

α -POX

In order to apply an anisotropic extinction correction, the raw intensities of Data Set 1 were reprocessed as previously described ($p=0.005$). The values of I and $\sigma(I)$ were corrected for Lorentz-polarization and absorption effects. The intensities of the two equiv-

Table 7. Final positional and thermal parameters for α -POX*

	10^4x	10^4y	10^4z	$10^4\beta_{11}$	$10^4\beta_{22}$	$10^4\beta_{33}$	$10^4\beta_{12}$	$10^4\beta_{13}$	$10^4\beta_{23}$
C(1)	-454 (2)	548 (3)	511 (1)	180 (3)	575 (11)	42 (1)	-10 (5)	22 (1)	-1 (2)
O(1)	848 (1)	-600 (3)	1481 (1)	246 (3)	1019 (10)	37 (1)	141 (4)	26 (1)	9 (2)
O(2)	-2201 (1)	2305 (2)	361 (1)	226 (3)	974 (10)	49 (1)	158 (4)	39 (1)	13 (2)
O(3)	-4512 (2)	-3849 (4)	1800 (1)	230 (4)	1007 (15)	46 (1)	104 (5)	35 (1)	22 (2)
H(1)	4643 (20)	4953 (43)	2913 (12)	305 (54)	1463 (183)	70 (14)	12 (78)	-76 (22)	-76 (43)
H(2)	588 (23)	1587 (45)	3795 (16)	281 (59)	1868 (238)	96 (17)	-200 (86)	51 (27)	-15 (49)
H(3)	-3869 (31)	4508 (52)	1584 (18)	608 (91)	1134 (252)	172 (25)	227 (110)	-75 (37)	210 (63)

* The anisotropic crystal Type II extinction correction was applied in this refinement.

addition to the usual structural parameters, were refined for 4 cycles. The values for R_1 and R_2 dropped to 3.6 and 4.4%, respectively. The final values for the components G_{ij} are given in Table 6.

A third refinement was carried out which included as variable parameters the six components G_{ij} of the tensor characterizing the anisotropic extinction in a Type II crystal. The initial values used were those derived for the α -DOX crystal. These six components, in addition to the usual structural parameters, were refined for 4 cycles yielding values of 2.8% and 3.9% for R_1 and R_2 respectively. The values for the components G_{ij} are included in Table 6. In the final cycle of all of the three above refinements, no shift in any parameter was larger than a standard deviation. No attempts were made to carry out refinements on a merged data set which would include intensities from Data Set 2.

A comparison of the R_2 values for the various models indicates that the anisotropic Type II refinement best characterizes the extinction in this particular crystal. The atomic positional and thermal parameters derived from the last cycle of the anisotropic Type II extinction are given in Table 7, along with the corresponding standard deviations in these parameters as derived from the inverse matrix. These parameters correspond to values for R_1 and R_2 (based on F) of 2.1% and 2.0% respectively. The values for $100|F_o|$ (corrected for extinction) and $100|F_c|$ (in electrons) are given in Table 8. The agreement in the positional parameters among all of the various refinements is comparable with that for α -DOX.

It is interesting to compare the extinction parameters given in Tables 3 and 6 for the α -DOX and α -POX crystals respectively. The form of the anisotropic extinction coefficient for a Type II crystal is $g = (M'GM)^{-1/2}$. The anisotropy of the extinction appears to be very similar for both crystals, with the G_{22} component being the largest in both cases. The vector component is largest for those planes whose normals have a large component in the direction of the b axis. Therefore, the extinction coefficient will be largest for $h0l$ reflections. The mosaic spread and particle size corresponding to the diagonal elements of the non-diagonalized tensor G provide some idea of mosaic spread and particle size and their anisotropies. The values of \bar{r} (in direction \mathbf{i}) = $10^{-4}\lambda G_{ii}^{1/2}$ are given in Table 9 for α -POX and α -DOX. The mean domain radius is much smaller near the b direction than in directions lying near the ac plane. This treatment should not be interpreted as giving a

Table 9. Mean domain shapes for the α -POX and α -DOX crystals

	α -POX	α -DOX
\bar{r} (in direction 1)*	10.34	7.63
\bar{r} (in direction 2)	3.34	3.86
\bar{r} (in direction 3)	11.90	7.41

* The values of \bar{r} , in centimeters, have been multiplied by 10^5 .

completely true picture of the mosaic structure because of the gross approximations made in this model. Nevertheless, these results do show that extinction can be anisotropic, and corrections for this anisotropy can be important.

In difference maps computed after isotropic extinction corrections the highest features for both α -POX and α -DOX were about $0.16 \text{ e.}\text{\AA}^{-3}$ in the centers of the C-C bonds. Maps computed after anisotropic extinction corrections no longer show these features, and show no density greater than about $0.1 \text{ e.}\text{\AA}^{-3}$. The disappearance of the residual density in the middle of the C-C bond may be due to a change in atomic scattering factors in going from the isotropic to anisotropic extinction correction or it may be due to this correction itself. Obviously the introduction of additional parameters in the anisotropic extinction model will tend to reduce the features of a residual density map. Nevertheless, as discussed in the last paper in this series, the differences between $|F_o|$ and $|F_c|$ after the anisotropic extinction correction are interpretable in terms of bonding effects.

Discussion

The results of this study confirm the general structural features of α -POX as described by previous investigators. The bond lengths and angles for both α -POX and α -DOX are given in Tables 10 and 11, respectively, along with the values obtained from the recent neutron diffraction studies of Sabine *et al.* (1969) and Coppens & Sabine (1969). The X-ray diffraction values for the O-H and O-D bond distances are consistently shorter than those found in the neutron diffraction studies. The corresponding X-ray and neutron diffraction values for bonds involving only the heavy atoms agree very well except for those which include the hydroxylic oxygen atom. Possible explanations for these differences will be offered later.

Perspective drawings of the structures of α -POX and α -DOX as viewed down the b axis are shown in Figs. 1 and 2 respectively. These Figures also display the labeling system for the various atoms. (These drawings were plotted with Johnson's program *ORTEP*. The scale represents a 50% probability contour for the thermal ellipsoids.) Discrete water molecules and oxalic acid molecules are linked together by a three-dimensional network of hydrogen bonds. The structures of α -POX and α -DOX are essentially identical except for differences in the corresponding OHO and ODO distances.

The oxalic acid molecule

The oxalate fragment is completely planar. The equation of the best least-squares plane through the carbon and oxygen atoms for each substance is given in Table 12. The deviation of each atom from the plane is also included. Including hydrogen (deuterium), the oxalic acid molecule has a crystallographic center of symmetry which lies between the two atoms. The distances of the hydrogen and deuterium atoms from the plane are

only 0.016 and 0.029 Å so that the whole acid molecule is essentially planar. The (COO)₂ group has also been found to be planar in β -deuteriooxalic acid dideuterate (Iwasaki & Saito, 1967), α -anhydrous oxalic acid (Cox,

Dougill, & Jeffrey, 1952), sodium oxalate (Jeffrey & Parry, 1952), lithium oxalate (Beagley & Small, 1964), and nearly planar in potassium oxalate monohydrate (Hodgson & Ibers, 1969). In contrast the two carboxyl

Table 10. Final bond lengths for α -POX and α -DOX

Bond	α -POX		α -DOX	
	X-ray*	Neutron†	X-ray‡	Neutron§
C(1)–C(1')	1.538 (2) Å	1.536 (3) Å	1.537 (2) Å	1.539 (2) Å
C(1)–O(1)	1.285 (1)	1.291 (5)	1.287 (1)	1.291 (2)
C(1)–O(2)	1.212 (1)	1.212 (4)	1.209 (1)	1.208 (2)
O(1)–H(1)	0.89 (2)	1.026 (7)	0.86 (2)	1.031 (2)
O(3)–H(2)	0.84 (2)	0.964 (7)	0.83 (2)	0.954 (2)
O(3)–H(3)	0.79 (3)	0.956 (9)	0.78 (2)	0.954 (2)
H(1)···O(3'')	1.63 (2)	1.480 (7)	1.67 (2)	1.493 (2)
H(2)···O(2'')	2.03 (2)	1.917 (8)	2.05 (2)	1.939 (2)
H(3)···O(2)	2.17 (2)	1.979 (9)	2.21 (2)	2.008 (2)
O(1)···O(3'')	2.512 (1)	2.506 (4)	2.531 (1)	2.524 (2)
O(3)···O(2'')	2.864 (2)	2.864 (5)	2.880 (2)	2.879 (2)
O(3)···O(2)	2.883 (1)	2.881 (4)	2.907 (1)	2.906 (2)

* These values are derived from the parameters in Table 7.

† These values are those of Sabine *et al.* (1969).

‡ These values are derived from the parameters in Table 4.

§ These values are those of Coppens & Sabine (1969).

Table 11. Final bond angles for α -POX and α -DOX

Bond	α -POX		α -DOX	
	X-ray*	Neutron†	X-ray‡	Neutron§
O(1)–C(1)–O(2)	126.8 (1)°	126.6 (3)°	126.8 (1)°	126.6 (1)°
O(1)–C(1)–C(1')	112.1 (1)	112.4 (3)	111.8 (1)	112.2 (1)
O(2)–C(1)–C(1')	121.1 (1)	121.0 (3)	121.4 (1)	121.2 (1)
C(1)–O(1)–H(1)	114.3 (8)	114.4 (6)	113.8 (8)	112.8 (1)
H(2)–O(3)–H(3)	101.5 (15)	105.9 (7)	101.2 (17)	105.8 (2)
O(1)–H(1)···O(3'')	177.4 (15)	179.3 (6)	176.3 (15)	177.4 (1)
H(1)···O(3'')–H(2'')	113.6 (10)	112.8 (7)	113.7 (10)	113.7 (1)
H(1)···O(3'')–H(3'')	112.0 (7)	117.6 (4)	110.7 (7)	119.2 (1)
O(3)–H(2)···O(2'')	171.0 (13)	166.9 (6)	172.0 (13)	167.7 (2)
H(2)···O(2'')–C(1''')	124.8 (4)	122.8 (6)	125.2 (4)	123.1 (1)
O(3)–H(3)···O(2)	150.2 (19)	156.6 (7)	148.9 (20)	156.0 (2)
H(3)···O(2)–C(1)	130.9 (4)	129.5 (7)	131.0 (4)	129.6 (1)

* These values are derived from the parameters in Table 7.

† These values are those of Sabine *et al.* (1969).

‡ These values are derived from the parameters in Table 4.

§ These values are those of Coppens & Sabine (1969).

Table 12. Best weighted-least-squares plane through the oxalate fragment*

	Atoms	A	B	C
α -POX	C(1), O(1), O(2), C(1'), O(1'), O(2')	3.132	3.077	–0.5445
α -DOX	C(1), O(1), O(2), C(1'), O(1'), O(2')	3.144	3.081	–0.5439

Distances in Å, of atoms from the plane†

	α -POX	α -DOX
C(1)	–0.0013	–0.0018
O(1)	0.0004	0.0005
O(2)	0.0004	0.0006
H(1)	0.0163	0.0289
C(1')	0.0013	0.0018
O(1')	–0.0004	–0.0005
O(2')	–0.0004	–0.0006
H(1')	–0.0163	–0.0289

* Equations of planes are of the form: $AX+BY+CZ=0$ in monoclinic coordinates.

† The estimated average standard deviation is about 0.0010 Å.

groups are rotated by 26.6° about the carbon-carbon bond in ammonium oxalate monohydrate (Robertson, 1965). In both α -POX and α -DOX the two C-O distances in the carboxyl group are distinctly different. The bond between carbon and the oxygen atom not involved in hydrogen bonding [C(1)-O(2)] is shorter than the one between carbon and the hydrogen bonded oxygen atom [C(1)-O(1)] by an average value of $0.076(1) \text{ \AA}$. The neutron diffraction value for the hydroxyl O-D bond length of $1.031(2) \text{ \AA}$ appears not to be significantly different from the corresponding O-H distance of $1.026(7) \text{ \AA}$.

The hydrogen bonding

In α -POX the oxygen atom of the water molecule is an acceptor for a strong hydrogen bond (O1)-H(1) . . . O(3'') (2.512 \AA) with the hydroxyl oxygen of the oxalic acid molecule. The hydrogen atom is completely associated with the hydroxyl oxygen atom as no evidence was found for any disordering of the hydrogen position or the existence of an H_3O^+ ion. The O(1)-H(1) . . . O(3'') angle of 179.3° indicates that the hydrogen atom lies very close to the line joining O(1) and O(3). The weaker O(3)-H(2) . . . O(2'') (2.864 \AA) and O(3)-H(3) . . . O(2) (2.883 \AA) hydrogen bonds are far from linear (166.9 and

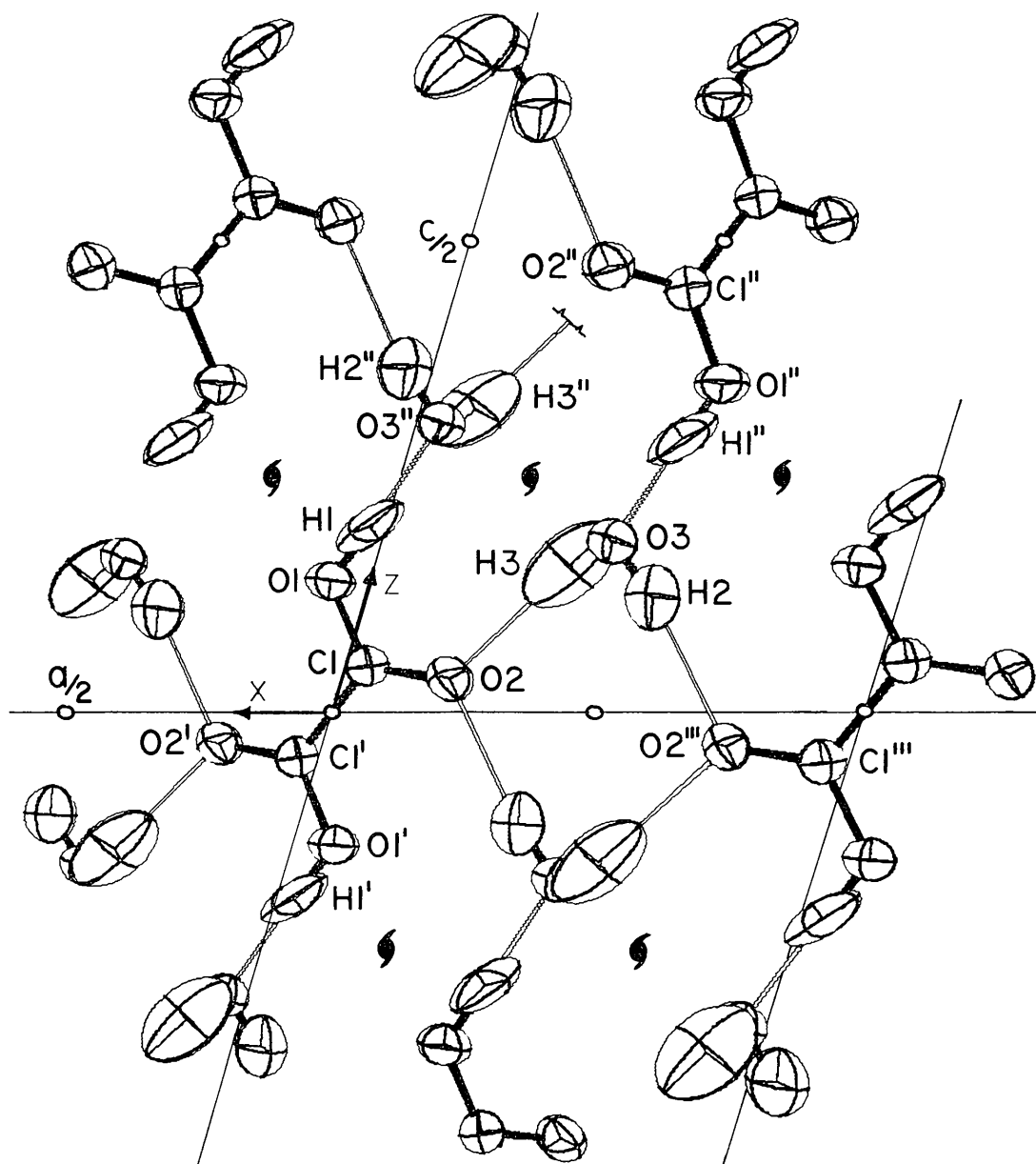


Fig. 1. Perspective view of α -POX along the b axis. The bond terminated indicates that the atom H(3'') is hydrogen bonded to an oxygen atom that is displaced one unit-cell along the negative b axis from O(2'').

156.6° respectively). These two hydrogen bonds form closed quadrilaterals which connect adjacent oxalic acid molecules. Infinite helical chains of hydrogen bonds extend up the b axis. The sequence of the chain is ... H(3'')-O(3'')... H(1)-O(1)-C(1)-O(2)... H(3)-O(3)... H(1'')-O(1'')-C(1'')-O(2'')... where O(2'') is hydrogen-bonded to a hydrogen atom displaced one unit-cell up the b axis from the starting point, H(3'').

The neutron values for the O-H bonds lengths in the water molecule (0.964 and 0.956 Å) are the same as those in gaseous water (0.96 Å). The H(2)-O(3)-H(1) angle of 105.9° is not significantly different from the value of 104.5° for water vapor.

Effects of extinction on bond lengths and bond angles

Selected bond lengths for some of the various extinction models are compared in Tables 13 and 15 for α -POX and α -DOX respectively. Corresponding selected bond angles are compared in Tables 14 and 16. Even though the agreement among the corresponding positional parameters for the various extinction models is good, small systematic differences in these parameters could introduce significant differences in bond lengths and angles. The largest differences that exist in corresponding values between any two sets are about twice the combined standard deviations. The values for the C(1)-C(1') and C(1)-C(2) distances in α -POX

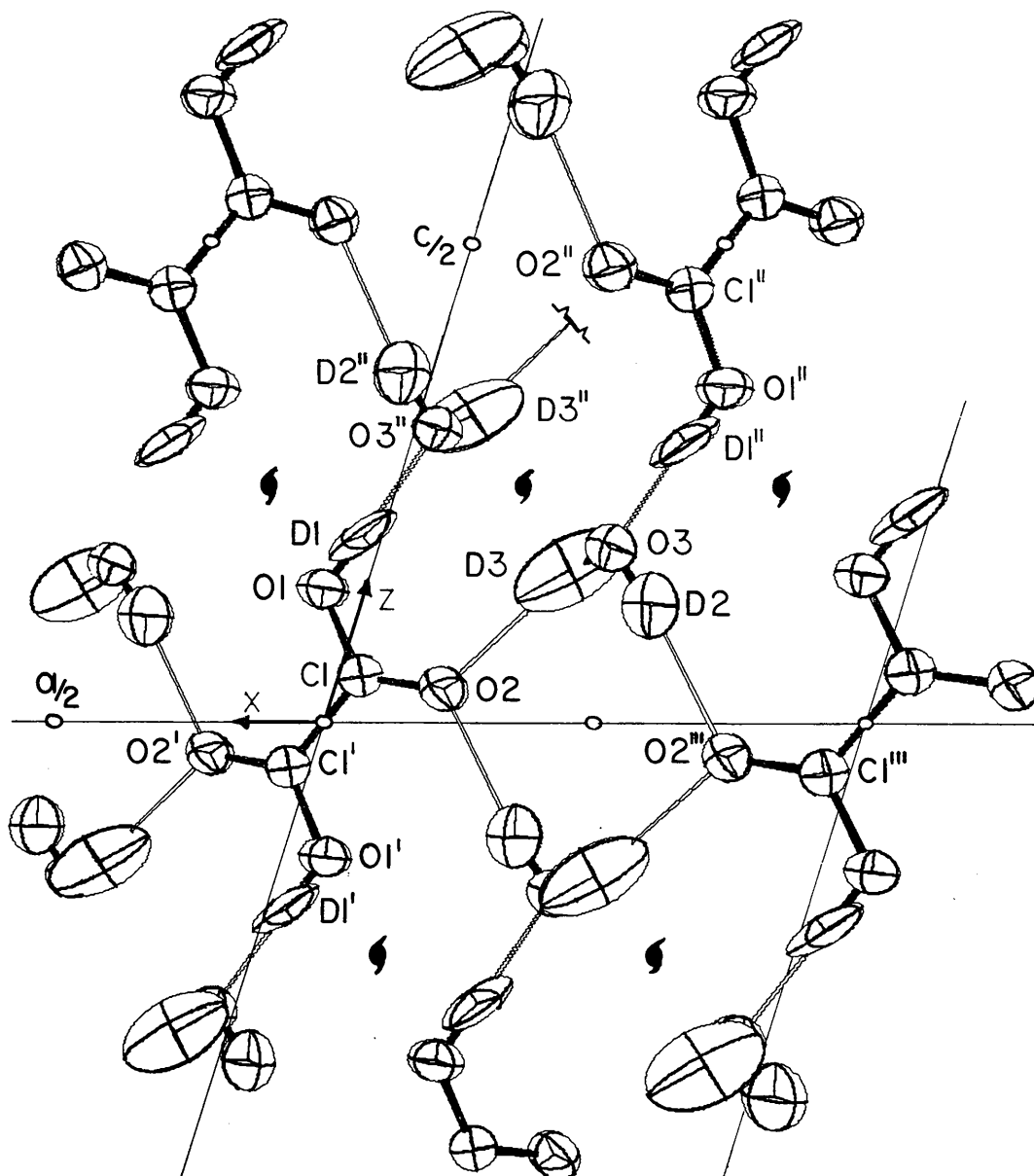


Fig. 2. Perspective view of α -DOX along the b axis.

for the merged data set are significantly different from those of the final anisotropic type II extinction refinement. They also differ somewhat from the values of the other refinements. The agreement among the corresponding values for α -DOX is much better. For the α -POX merged data set, the procedure of separately correcting two sets of data for extinction and then merging them is a possible source for systematic errors.

The corresponding X-ray and neutron values for the bond lengths involving only the heavy atoms agree

very well. Exceptions are those bonds which involve the atom O(1). The X-ray and neutron values for the z coordinate of O(1) differ by 0.008 Å for both substances. This shortens the C(1)–O(1) bond and lengthens the O(1)–O(3'') distance relative to the corresponding neutron values. At present, these differences are poorly understood and are attributed to either systematic errors in some or all of the experiments or to bonding effects. This will be discussed in greater detail in the fourth paper in this series (Coppens *et al.*, 1969).

Table 13. Comparison of bond lengths in α -POX for various extinction models

Bond	No correction	Zachariasen correction	Merged data set	Anisotropic Type I correction	Anisotropic Type II correction
C(1)–O(1')	1.543 (6) Å	1.545 (3) Å	1.546 (2) Å	1.539 (2) Å	1.538 (2) Å
C(1)–O(1)	1.284 (4)	1.284 (2)	1.281 (2)	1.285 (1)	1.285 (1)
C(1)–O(2)	1.210 (4)	1.208 (2)	1.207 (2)	1.212 (1)	1.212 (1)
O(1)–H(1)	0.98 (6)	0.94 (3)	0.82 (4)	0.89 (2)	0.89 (2)
O(3)–H(2)	0.93 (6)	0.83 (3)	0.81 (3)	0.82 (2)	0.84 (2)
O(3)–H(3)	0.74 (7)	0.82 (3)	0.80 (3)	0.80 (2)	0.79 (3)
O(1)–O(3'')	2.507 (4)	2.507 (2)	2.510 (2)	2.512 (2)	2.512 (1)
O(3)–O(2'')	2.867 (4)	2.870 (2)	2.869 (2)	2.865 (2)	2.864 (2)
O(3)–O(2)	2.887 (3)	2.883 (2)	2.884 (2)	2.883 (1)	2.883 (1)

Table 14. Comparison of bond angles in α -POX for various extinction models

Bond	No correction	Zachariasen correction	Merged data set	Anisotropic Type I correction	Anisotropic Type II correction
O(1)–C(1)–O(2)	126.9 (3)°	126.9 (3)°	127.1 (1)°	126.8 (1)°	126.8 (1)°
O(1)–C(1)–C(1')	112.1 (3)	112.0 (2)	111.9 (1)	112.0 (1)	112.1 (1)
O(2)–C(1)–C(1')	121.0 (3)	121.1 (2)	121.0 (1)	121.1 (1)	121.1 (1)
O(1)–H(1)–O(3'')	176.0 (38)	178.3 (18)	175.7 (22)	176.4 (17)	177.4 (15)
O(3)–H(2)–O(2'')	175.3 (38)	170.8 (24)	169.0 (19)	171.4 (15)	171.0 (13)
O(3)–H(3)–O(2)	159.0 (61)	160.2 (28)	153.9 (21)	150.4 (21)	150.2 (19)

Table 15. Comparison of bond lengths in α -DOX for various extinction models

Bond	No correction	Zachariasen correction	Merged data set	Anisotropic Type I correction	Anisotropic Type II correction
C(1)–C(1')	1.540 (6) Å	1.543 (3) Å	1.541 (3) Å	1.538 (2) Å	1.537 (2) Å
C(1)–O(1)	1.285 (4)	1.286 (2)	1.283 (2)	1.287 (1)	1.287 (1)
C(1)–O(2)	1.210 (4)	1.207 (2)	1.209 (2)	1.209 (1)	1.209 (1)
O(1)–D(1)	0.89 (6)	0.91 (2)	0.88 (2)	0.85 (2)	0.86 (2)
O(3)–D(2)	0.91 (5)	0.82 (2)	0.84 (2)	0.83 (2)	0.83 (2)
O(3)–D(3)	0.70 (7)	0.79 (3)	0.70 (4)	0.77 (2)	0.78 (2)
O(1)–O(3'')	2.530 (5)	2.525 (2)	2.531 (2)	2.532 (1)	2.531 (1)
O(3)–O(2'')	2.880 (5)	2.882 (2)	2.876 (2)	2.879 (1)	2.880 (2)
O(3)–O(2)	2.910 (3)	2.908 (2)	2.908 (1)	2.907 (1)	2.907 (1)

Table 16. Comparison of bond angles in α -DOX for various extinction models

Bond	No correction	Zachariasen correction	Merged data set	Anisotropic Type I correction	Anisotropic Type II correction
O(1)–C(1)–O(2)	126.9 (3)°	126.9 (2)°	126.9 (1)°	126.8 (1)°	126.8 (1)°
O(1)–C(1)–C(1')	112.0 (3)	111.9 (2)	112.1 (2)	111.8 (1)	111.8 (1)
O(2)–C(1)–C(1')	121.1 (3)	121.2 (2)	121.0 (1)	121.4 (1)	121.4 (1)
O(1)–D(1)–O(3'')	175.1 (41)	177.7 (18)	171.4 (25)	175.5 (16)	176.3 (15)
O(3)–D(2)–O(2'')	175.6 (39)	170.3 (21)	171.7 (19)	171.5 (13)	172.0 (13)
O(3)–D(3)–O(2)	150.2 (19)	156.0 (22)	145.1 (31)	148.0 (21)	148.9 (20)

The isotope effect

All three crystallographically independent O—H...O bonds expand significantly with deuteration. The differences in the corresponding O—D...O and O—H...O distances are given in Table 17. The isotope effect is completely localized in the hydrogen bonds, as the bond lengths within the oxalate fragment remain invariant upon deuteration. The cell constants for both substances given previously in Table 1 agree with the directions and magnitudes of maximum and minimum expansion in the (010) projection of the unit cell originally found by Robertson & Ubbelohde (1939). Any changes in the *b* direction were not measured but were assumed to be small. They concluded that the changes in the lattice parameters were almost entirely due to an expansion of 0.041 Å in the strong O(1)—H(1)...O(3'') hydrogen bond since the direction of this bond is very near that of the maximum expansion. It was assumed that deuteration had little or no effect on the two weaker hydrogen bonds, even though the direction of the O(3)—H(3)...O(2) bond is essentially coincident with the direction of maximum expansion. The present results clearly indicate that this assumption is not valid as the largest expansion does in fact occur in this weak bond. There is also a significant expansion in the O(3)—H(2)...O(2'') distance, which lies near the direction of minimum expansion. Ubbelohde & Roberson originally reported a small contraction of -0.0001 per unit length in this bond. Deuteration has no significant effect on the angles of the two weak hydrogen bonds. The O(1)—H(1)...O(3'') angle appears to bend $1.9(6)^\circ$ with deuteration. This is accompanied by a slight decrease of $1.6(6)^\circ$ in the C(1)—O(1)—H(1) angle.

Table 17. *Isotope effect on hydrogen bond distances*

Bond	r_H	X-ray	$r_D - r_H$	Neutron
	X-ray			
O(1)...O(3'')	2.512 Å	0.019 (1) Å	0.017 (5) Å	
O(3)...O(2'')	2.864	0.016 (3)	0.018 (6)	
O(3)...O(2)	2.883	0.024 (1)	0.022 (5)	

These results clearly show that correlations of specific bond-length changes with changes in cell constants alone are unreliable for complex crystals such as α -POX which contain more than one crystallographically independent hydrogen bond per unit cell. Consequently, most of the current data on isotope effects may be in error and should be carefully checked by single-crystal diffraction techniques.

The sensitivity of hydrogen bonds to isotopic substitution has been theoretically interpreted by Gallagher (1959) to be due to the differences in zero-point energy distributions of hydrogen and deuterium in the O...O potential field. The isotope effect was attributed to be a function of hydrogen bond length. Large expansions were predicted for strong bonds which diminished as the O...O distance increased. However, this ignores cooperative effects that appear to exist in systems such as α -POX, which contain complex networks

of hydrogen bonds. Large isotope effects are not always localized in only the strongest hydrogen bonds, but may be spread throughout all of the hydrogen bonds in the crystal. Such effects are important and make it difficult to correlate directly the isotope effect with only hydrogen bond strengths in complex structures. Such considerations could alter conclusions that have been reached with regard to the structural effects of deuteration on the α -helix of proteins (Tomita, Rich, de Loze & Blout, 1962).

We wish to acknowledge the close cooperation we have enjoyed with P. Coppens and W. C. Hamilton during the course of this work. In particular R. G. D. wishes to acknowledge the hospitality extended him during an extended visit to Brookhaven National Laboratory where the calculations on anisotropic extinction were performed. This work was supported by the Advanced Research Projects Agency of the Department of Defense through the Northwestern Materials Research Center.

References

- AHMED, F. R. & CRUICKSHANK, D. W. J. (1953). *Acta Cryst.* **6**, 385.
 BEAGLEY, B. & SMALL, R. W. (1963). *Proc. Roy. Soc. A275*, 469.
 BUSING, W. R. & LEVY, H. A. (1957). *J. Chem. Phys.* **26**, 563.
 CHIBA, T. (1964). *J. Chem. Phys.* **41**, 1352.
 COPPENS, P. & HAMILTON, W. C. (1969). *Acta Cryst.* In the press.
 COPPENS, P., LEISEROWITZ, L. & RABINOVICH, D. (1965). *Acta Cryst.* **18**, 1035.
 COPPENS, P. & SABINE, T. M. (1969). *Acta Cryst.* **B25**, 2442.
 COPPENS, P., SABINE, T. M., DELAPLANE, R. G. & IBERS, J. A. (1969). *Acta Cryst.* **B25**, 2451.
 CORFIELD, P. W. R., DOEDENS, R. J. & IBERS, J. A. (1967). *Inorg. Chem.* **6**, 197.
 COX, E. G., DOUGILL, M. W. & JEFFREY, G. A. (1952). *J. Chem. Soc.* p.4854.
 DELAPLANE, R. G. & IBERS, J. A. (1966). *J. Chem. Phys.* **45**, 3451.
 FURNAS, T. C. (1957). *Single Crystal Orienter Instruction Manual*. Milwaukee: General Electric Co.
 GALLAGHER, K. J. (1959). In *Hydrogen Bonding*, p.45. Ed. D. HADZI. London: Pergamon Press.
 GARRETT, R. S. (1954). Oak Ridge National Laboratory Report No. 1745.
 HAMILTON, W. C. (1957). *Acta Cryst.* **10**, 629.
 HANSON, H. P., HERMAN, T., LEA, J. D. & SKILLMAN, S. (1964). *Acta Cryst.* **17**, 1040.
 HODGSON, D. J. & IBERS, J. A. (1969). *Acta Cryst.* **B25**, 469.
 IBERS, J. A. (1962). In *International Tables for X-ray Crystallography*, Vol. III, Table 3.3.1A. Birmingham: Kynoch Press.
 IBERS, J. A. (1965). *Ann. Rev. Phys. Chem.* **16**, 375.
 IWASAKI, F. F., IWASAKI, H. & SAITO, Y. (1967). *Acta Cryst.* **23**, 64.
 IWASAKI, F. F. & SAITO, Y. (1967). *Acta Cryst.* **23**, 56.
 JEFFREY, G. A. & PARRY, G. S. (1952). *J. Amer. Chem. Soc.* **76**, 5283.
 ROBERTSON, J. H. (1965). *Acta Cryst.* **18**, 410.

- ROBERTSON, J. M. (1936). *Proc. Roy. Soc. A* **157**, 79.
 ROBERTSON, J. M. & UBBELOHDE, A. R. (1938). *Proc. Roy. Soc. A* **167**, 122.
 ROBERTSON, J. M. & UBBELOHDE, A. R. (1939). *Proc. Roy. Soc. A* **170**, 222.
 ROBERTSON, J. M. & WOODWARD, I. (1936). *J. Chem. Soc.* p. 1817.
 ROBINSON, W. T. & IBERS, J. A. (1967). *Inorg. Chem.* **6**, 1208.
 SABINE, T. M., COX, G. W. & CRAVEN, B. M. (1969). *Acta Cryst.* **B25**, 2437.
 STEWART, R. F., DAVIDSON, E. R. & SIMPSON, W. T. (1965). *J. Chem. Phys.* **42**, 3175.
 TOMITA, K., RICH, A., DE LOZE, C. & BLOUT, E. R. (1962). *J. Mol. Biol.* **4**, 83.
 UBBELOHDE, A. R. & GALLAGHER, K. J. (1955). *Acta Cryst.* **8**, 71.
 UBBELOHDE, A. R. & WOODWARD, I. (1942). *Proc. Roy. Soc. A* **179**, 399.
 ZACHARIASEN, W. H. (1963). *Acta Cryst.* **16**, 1139.
 ZACHARIASEN, W. H. (1965). *Acta Cryst.* **18**, 705.
 ZACHARIASEN, W. H. (1968). *Acta Cryst.* **A24**, 212.

Acta Cryst. (1969). **B25**, 2437

A Neutron Diffraction Study of α -Oxalic Acid Dihydrate

BY T. M. SABINE AND G. W. COX

Materials Division, AEC Research Establishment, Lucas Heights, N.S.W., Australia

AND B. M. CRAVEN

Crystallography Laboratory, University of Pittsburgh, Pittsburgh, Pennsylvania 15213, U.S.A.

(Received 20 December 1968)

A determination of the crystal structure of α -oxalic acid dihydrate from three-dimensional neutron diffraction data has confirmed, with greater precision, the atomic parameters found previously from $h0l$ and $0kl$ data. Assumptions concerning the vibration state of the molecule are shown to introduce uncertainties in bond lengths much greater than the standard deviations derived from least-squares refinement of atomic parameters. The extent to which data collection at low temperature would reduce the uncertainty is calculated.

Introduction

The crystal structure of α -oxalic acid dihydrate (here abbreviated α -POX) has been investigated several times by X-ray diffraction methods. Ahmed & Cruickshank (1953) obtained the positions of the carbon and oxygen atoms by a re-examination of earlier two-dimensional data of Robertson & Woodward (1936) and Brill, Hermann & Peters (1942). Garrett (1954) carried out a neutron diffraction investigation and located the hydrogen atoms from $h0l$ and $0kl$ data.

The present three-dimensional neutron structure determination has been carried out in order to obtain more precise atomic parameters (particularly for the hydrogen atoms), to examine the effects of assumptions about the atomic anisotropic thermal motions on the observed bond lengths, and to enable a more complete comparison between X-ray and neutron diffraction studies of this material (α -POX, Delaplane & Ibers, 1969), and the two deuterated crystalline forms (α -DOX and β -DOX, Coppens & Sabine, 1969).

Experimental

The crystals of oxalic acid dihydrate were obtained from Dr A. McL. Mathieson of the Division of Chemical Physics, C.S.I.R.O., Melbourne.

The crystal data (from Delaplane & Ibers, 1969) are:

Space group $C_{2h}^5 - P2_1/n$,
 $a = 6.119$, $b = 3.607$, $c = 12.057$ Å, $\beta = 106^\circ 19'$, $Z = 2$.

Two crystals were used, one of mass 36.65 mg and one of mass 2.75 mg. Most of the data were obtained from the larger crystal which was pillar shaped with well developed $\{101\}$, $\{10\bar{1}\}$ and $\{001\}$ forms. The small crystal was cut to a rough cube.

Data collection

The data were collected on two single-crystal diffractometers installed on the reactor HIFAR. For these instruments the respective fluxes and wave lengths of the monochromatic neutron beam at the specimen are 2.8×10^5 n cm⁻² sec⁻¹ at 1.10 Å, and 6×10^6 n cm⁻² sec⁻¹ at 1.09 Å.

The large crystal was mounted on a two-circle goniometer with c^* along the ϕ axis so that a ϕ -rotation would present maximum and minimum path lengths for the incident and diffracted beams of $00l$ reflections and enable extinction and absorption effects to be detected. Both effects were apparent. However, the integrated intensities $00l$ observed at a ϕ -setting half way between the minimum and maximum neutron path length positions were 30 per cent larger than those